

Blueschist-to-greenschist transition and the *P-T* path of prasinites from the Lavrion area, Greece

EMMANUEL BALTATZIS

National University of Athens, Department of Geology, Panepistimiopolis-Ano Ilissia, Athens 15784, Greece

Abstract

The Lavrion area is part of the Attic-Cycladic massif. Blue amphibole analyses revealed that they are glaucophane or ferroglaucophane. Ca-amphiboles are characterized as actinolite or actinolitic hornblende. The Ps component of epidotes from the glaucophane-bearing rocks varies from 25.42–30.89%, whereas the Ps component of epidotes from the greenschist assemblages ranges from 23.81–26.88%. Chlorites show narrow compositional variations of ferromagnesian ratios ($X_{mg}=0.48-0.53$). Albites are almost pure Ab₁₀₀. The K-feldspar present has a low Ab content. The evolution of the prasinites studied is characterized by the progressive transformation of eclogite facies (?) rocks through epidote blueschist facies into greenschists. A *P-T* path for the prasinites is presented indicating epidote blueschist facies at *P-T* conditions of around 7.0–7.5 kbar and 300–340°C. Pressures of 4.0–4.5 kbar and temperatures around 340–360°C are estimated for the subsequent overprint in the greenschist facies. The path EBS to GS conditions followed under nearly isothermal uplift.

KEYWORDS: blueschist, greenschist, prasinite, *P-T* path, Lavrion, Greece.

Introduction

THE co-existence of blueschists and greenschists in the same rock units has been reported from many areas the world over (Moore, 1984; Brown, 1986; Bröcker, 1990). The close spatial association of blueschist facies rocks and their greenschist facies derivatives is also well known from numerous high-pressure terranes which have suffered subsequent low to medium pressure overprinting. Most workers have ascribed the preservation of relic pressure assemblages to rapid uplift and sluggish reaction kinetics.

The blueschist unit of the Cyclades, Greece, is dominated by the formation of Eocene blueschist and eclogite facies rocks which are preserved in the island of Sifnos, Syros and Tinos (Dürr *et al.*, 1978; Altherr *et al.*, 1979; Bröcker, 1990). During exhumation in the late Oligocene to early Miocene a major tectonic overprint occurred throughout the massif, which partially or completely effaced the assemblages of the Eocene high-pressure metamorphism (Andriessen *et al.*, 1979; Altherr *et al.*, 1982; Schliestedt *et al.*, 1987; Bröcker, 1990; Avigad and Garfunkel, 1991; Avigad *et al.*, 1992). Greenschist facies conditions

were regionally typical of this metamorphic phase. The greenschist overprint was followed in the early Miocene by extensive emplacement of granitoid rocks with local contact metamorphism (Baltatzis, 1981; Salemink, 1985).

This study focuses on the mineralogy, petrochemistry and *P-T* path of prasinites rock samples of the Lavrion area, Greece (Fig. 1).

Local geologic setting

The Lavrion area is part of the Attic-Cycladic Massif of SE Greece. The first systematic geological and petrological survey of Attica was carried out by Lepsius (1893). The petrography of the Lavrion area and the related mineralization have been described by Marinos and Petrascheck (1956). The mineralogy and the physical conditions of metamorphism of a calc-silicate hornfels have been described by Baltatzis (1981). The structural and deformational events and metamorphic development of Pentelikon, Hymetus and Lavrion to Attic-Cycladic crystalline complexes have been investigated more recently by Kessel (1990).

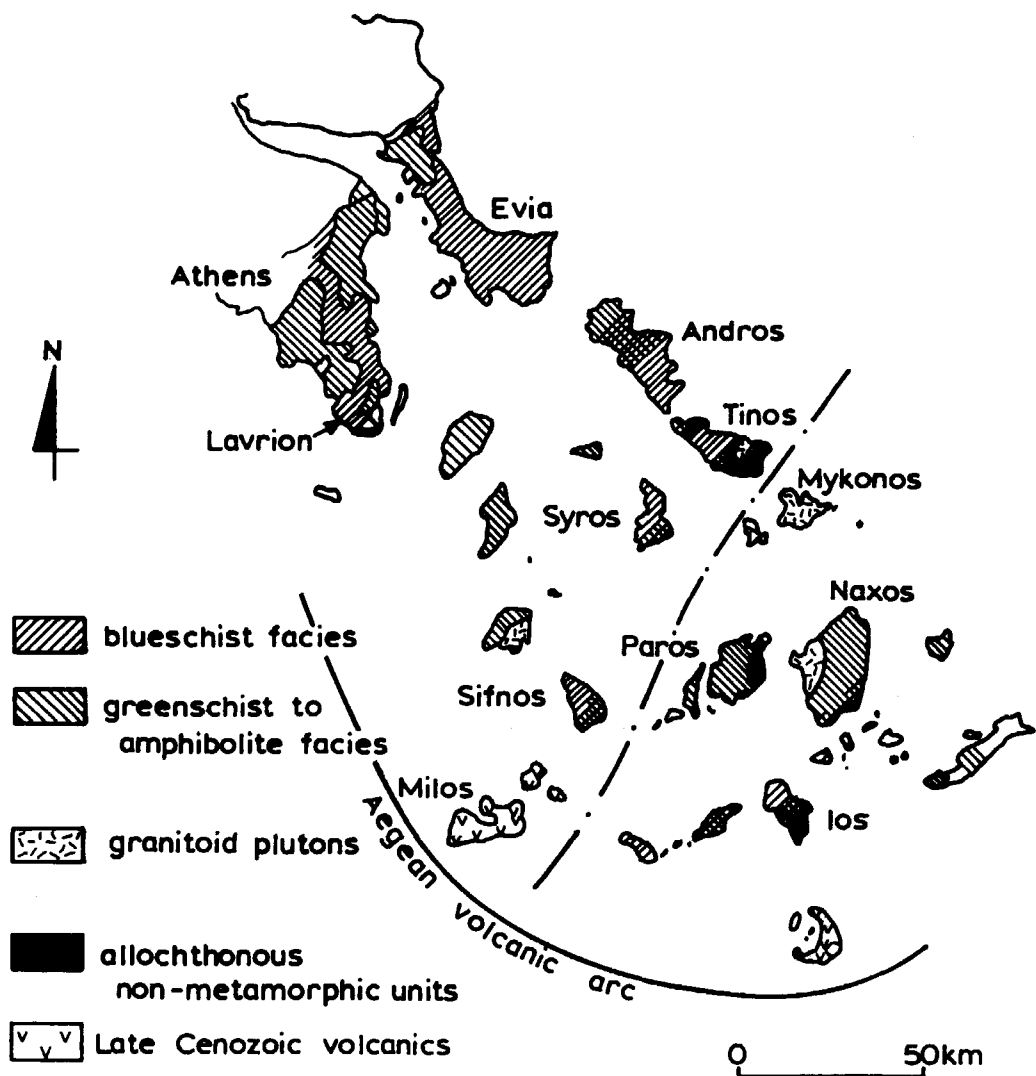


FIG. 1. Geological setting of the Cycladic blueschist belt. The rocks in the north-west part of the Cyclades have isothermal cooling decompression paths, whereas exposures in the eastern part of the massif show significant heating. The dash-dot line on figure marks the limit between the two domains. The (Δ) shows the locality of the collected samples.

Petrography

Thin section studies and electron microprobe analyses reveal the presence of a number of minerals including Na-amphiboles-epidote-Ca-amphiboles-albite-chlorite \pm muscovite \pm biotites \pm oxides. Glaucophane usually shows euhedral forms. No inclusions are recognized in glaucophane. The

glaucophane in some samples is mantled by a calcic-sodic amphibole suggesting stable co-existence of both minerals, or, in some samples, is rimmed by chlorite. Calcic amphiboles are abundant and occur as acicular crystals in the greenschist facies assemblages.

Epidote/clinozoisite are dispersed throughout the thin sections and show euhedral and subhedral forms.

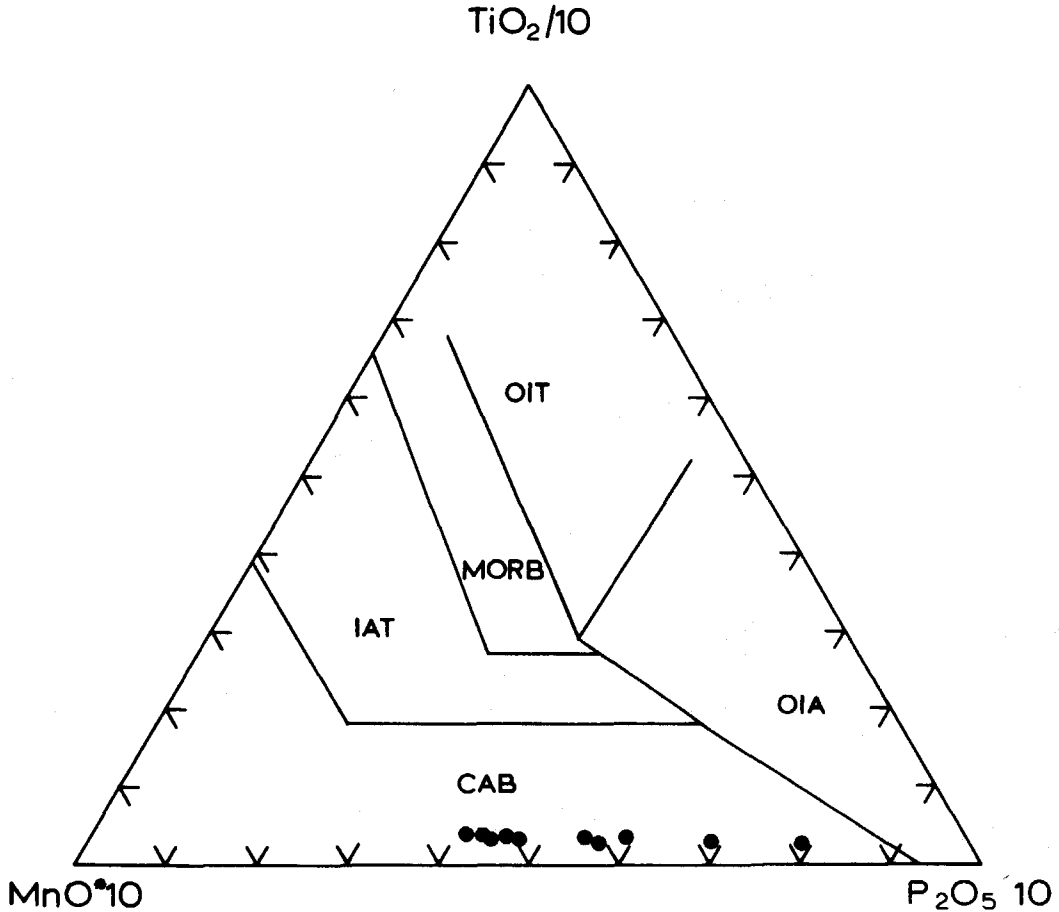


FIG. 2. MnO-TiO₂-P₂O₅ discrimination diagram (after Mullen, 1983). Prasinites plot in the island arc calc-alkaline basalt field (CAB).

Chlorites are present in the matrix and they often surround glaucophane, suggesting reaction relationships between chlorites and glaucophane. Albites show anhedral forms and are untwinned. Very few muscovite and biotite crystals are present in the two rock types.

Geochemistry of prasinite

The prasinites studied have been analysed for major and trace elements by X-ray fluorescence analysis using a Philips PW 1450 spectrometer; details of the technique used and the correction procedures involved have been described by Brown *et al.* (1973). The analyses along with the mineral assemblages are given in Table 1. The composition of the prasinites from

Lavrion range from basalts to trachyandesites. Using major and incompatible trace element discrimination diagrams (Figs 2 and 3), it can be shown that the prasinites studied plot in the calc-alkaline basalt field (MnO-TiO₂-P₂O₅) and in the volcanic arc basalts (Zr-Nb-Y). As is shown in the MORB normalized diagrams of the rocks studied (Fig. 4) there is an enrichment in LIL elements which is in accordance with their calc-alkaline affinity. The LIL/HFS ratio for all the samples seems to be the same. The increasing concentration of all the elements shows fractional crystallization of a common parent magma. Therefore it is most likely that their igneous precursors were found in an island-arc environment. Furthermore, if we compare our data with data from Sifnos and Kithnos (Fig. 4 of Schliestedt *et al.*, 1994), eclogites

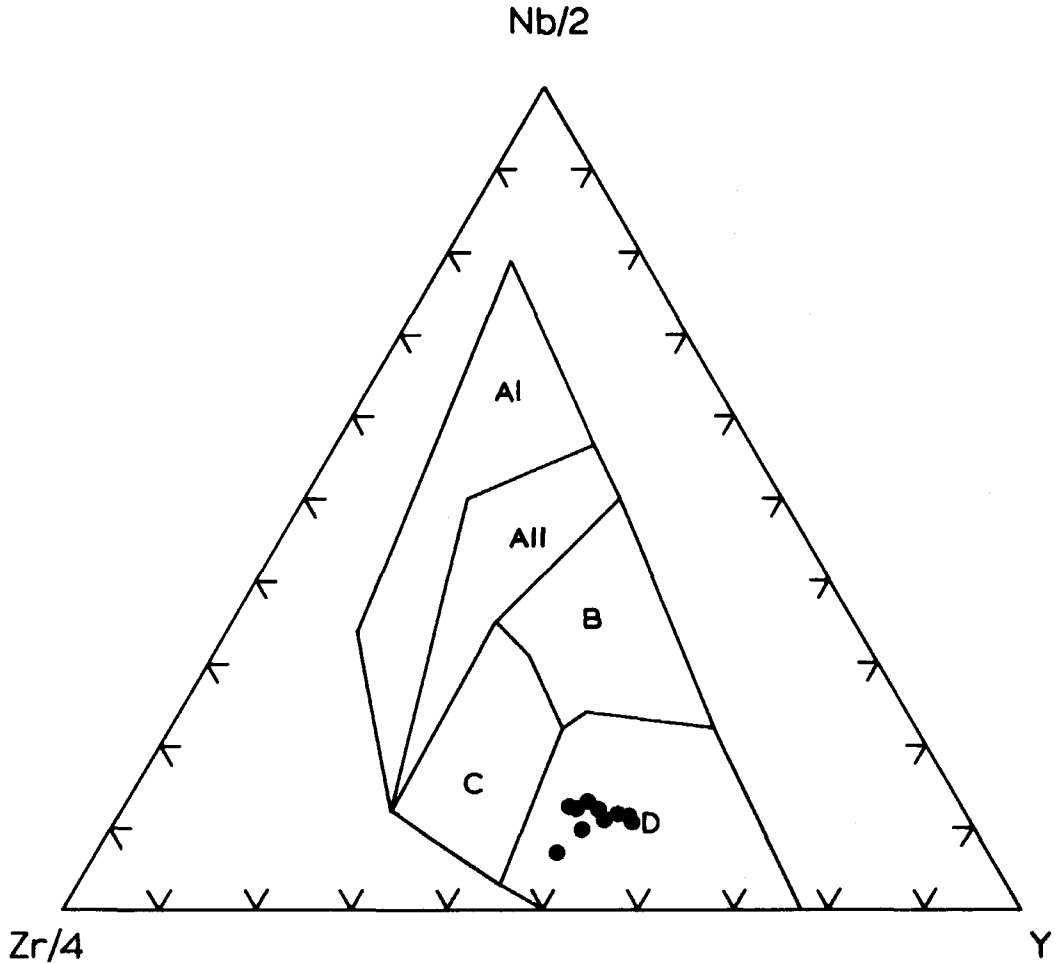


FIG. 3. The Zr–Nb–Y discrimination diagram for basalts (after Meschede, 1986). The prasinites plot in the volcanic arc basalts (D).

from Sifnos and alkalic greenschist from Kithnos show higher incompatible element enrichment from the prasinites studied.

Mineral chemistry

Mineral analyses (Tables 2,3,4 and 5) were performed at the University of Manchester, using a Cambridge Instrument Geoscan fitted with a Link Systems model ZAF-4/FLS quantitative analysis software system. Operating conditions were 15 kV accelerating voltage and 3 nA specimen current on cobalt metal. Accuracy, precision and detection limits of energy dispersive electron microprobe

analyses of silicate are given by Dunham and Wilkinson (1978).

Analyses of amphiboles and their structural formulae are listed in Table 2. Sodic amphiboles are ferro-glaucophane or glaucophane (L1 and S4) similar to sodic amphiboles in HP metabasites from the Attic-Cycladic complex (Schliestedt, 1986; Schliestedt *et al.*, 1994). No zonation has been observed in the sodic amphiboles. Calcic amphiboles are actinolite or actinolitic hornblende (S3). The analyses of epidotes are listed in Table 3 and recalculated to the formula $X_4Y_6(\text{Si,Al})_6\text{O}_{24}(\text{OH})_2$, assuming all Fe to be present as Fe_2O_3 . In the glaucophane-bearing rocks (samples L1, L3) the

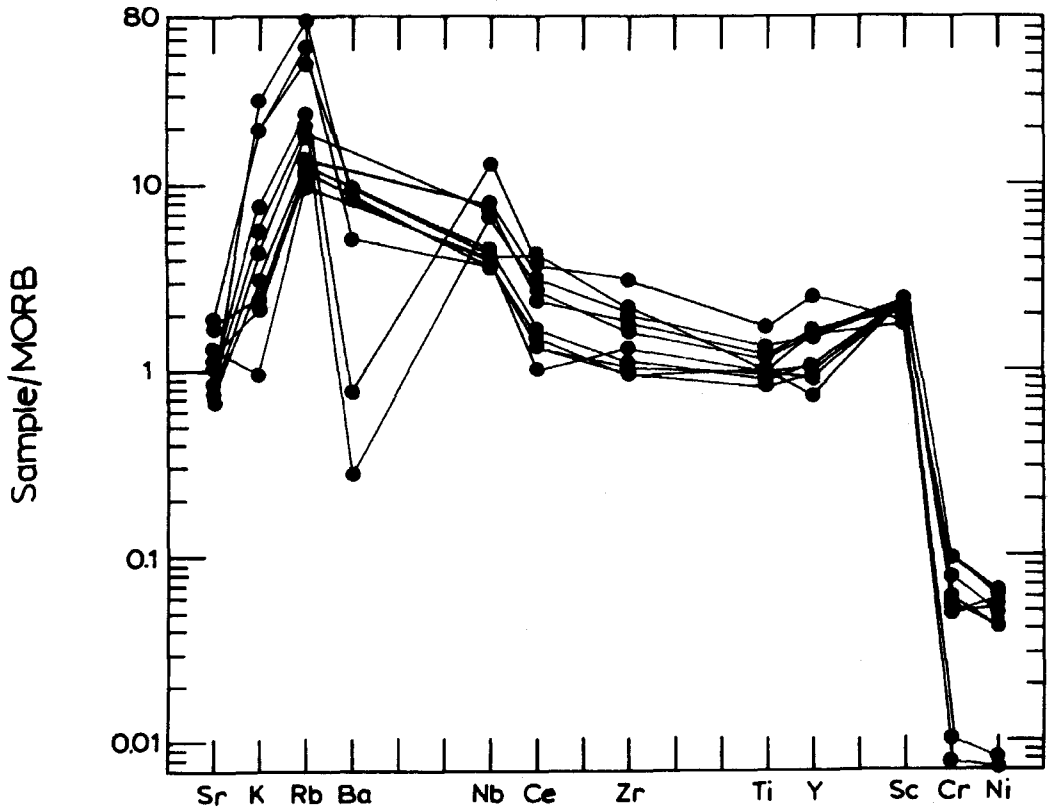


Fig. 4. MORB-normalized minor and trace elements patterns of prasinites. Normalizing values from Pearce (1983).

clinozoisite component ranges from 73.80–69.11%, and the pistacite component from 25.42–30.89%. Epidote in the greenschist assemblages (samples L4, L5) has a clinozoisite component from 73.12–76.19%, while the pistacite component is 26.88–23.81%, typical of other greenschist facies metabasites (Bröcker, 1990; Schliestedt *et al.*, 1994). Analyses of chlorites (Table 4) of the rocks studied show narrow compositional variation $X_{mg} = 0.48–0.53$ and 2.77–3.04 Si per formula unit (pfu), which is typical of chlorite from other greenschist facies metabasites from the Cyclades islands (Schliestedt *et al.*, 1994). Albites are nearly always pure Ab_{100} (Table 5). K-feldspar has a low albite content ($Or_{98.19} Ab_{1.81} An_{0.0}$).

Thermobarometry and *P-T* path of the prasinites studied

The relationships between eclogite facies, epidote-blueschist facies and greenschist facies rocks are

made more evident by the recent calculations of Evans (1990). Figure 5 shows the facies boundaries defining the stability of epidote-blueschist facies for sodic amphibole which are glaucophane to ferroglaucophane (Leake, 1978). Assemblages equilibrating in the epidote-blueschist facies are recognized in the prasinites studied. Neither omphacite nor garnet are found in these rocks and the glaucophane-albite-epidote paragenesis is indicative of minerals formed within the albite-bearing region of the epidote-blueschist facies. The possible reaction denoted by the first appearance of glaucophane in the rocks studied is: omphacite + garnet + $H_2O \rightarrow$ glaucophane + epidote-quartz.

In view of previous evidence showing that eclogites are overprinted by epidote-blueschist facies assemblages it is very likely that all epidote-blueschist facies (samples L1, L3) rocks evolved through the retrogression of eclogites during exhumation (Avigad *et al.*, 1992). Metabasic epidote-blueschist were further transformed into

TABLE 1. XRF bulk rock analyses of representative prasinites and their mineral assemblages

	L1	L3	BR1	L1X	L1Y	L4	L5	S1X	S3	S4
SiO ₂	47.15	53.80	43.39	47.25	48.07	44.45	48.30	41.42	46.90	47.88
TiO ₂	1.84	2.60	1.50	2.02	1.72	1.45	1.34	1.46	1.48	1.23
Al ₂ O ₃	12.33	11.25	14.66	12.40	13.20	10.83	12.35	11.26	11.70	12.94
Fe ₂ O ₃	6.70	8.47	6.23	5.94	6.54	4.67	4.38	6.10	6.70	5.48
FeO	9.39	4.95	4.49	9.11	8.28	7.65	6.55	7.05	6.19	5.36
MnO	0.19	0.18	0.21	0.19	0.20	0.20	0.20	0.21	0.20	0.19
MgO	9.74	3.65	4.34	9.63	9.04	9.10	9.27	9.28	7.33	8.57
CaO	5.32	6.18	12.01	5.66	5.15	13.22	10.91	13.28	8.77	8.70
Na ₂ O	2.88	5.14	3.13	3.13	3.18	2.84	2.85	2.57	2.58	2.38
K ₂ O	0.50	0.88	2.27	0.36	0.65	0.25	0.28	0.11	3.23	2.21
P ₂ O ₅	0.30	0.77	0.29	0.46	0.26	0.18	0.19	0.17	0.15	0.16
CO ₂	0.04	0.97	5.42	0.02	0.02	2.90	0.54	3.76	2.46	1.57
H ₂ O	4.08	1.36	2.86	3.96	4.08	2.55	2.54	3.09	2.61	3.42
Total	100.46	100.20	100.79	100.13	100.39	100.29	99.97	100.46	100.30	100.09
Nb	26	47	15	28	24	13	16	14	13	13
Zr	166	277	198	183	149	93	101	120	86	86
Y	54	86	53	52	56	31	36	36	25	33
Sr	91	126	230	88	107	141	215	166	84	106
Rb	21	27	50	15	23	13	14	11	85	62
Zn	152	140	78	136	159	99	88	109	121	79
Cu	92	30	6	92	106	99	94	111	164	96
Ni	86	17	15	87	105	110	132	123	111	136
Cr	181	31	23	166	230	152	293	149	148	295
Ce	29	45	51	38	32	16	20	12	18	16
Nd	18	34	33	20	19	7	16	8	8	5
V	297	125	168	294	281	247	244	278	270	243
La	9	8	26	11	8	1	8	10	6	6
Ba	0	11	136	0	4	0	0	0	118	73
Sc	39	31	30	37	35	42	41	39	41	42
Quartz	X	X	X	X	X	X	X	X	X	X
Albite	X	X	X	X	X	X	X	X	X	X
Na-amph.	X	X	—	X	X	—	—	X	X	X
Ca-amph.	—	—	—	X	X	X	X	X	X	X
Epidote	X	X	X	X	X	X	X	X	X	X
Chlorite	X	X	X	X	X	X	X	X	X	X
Calcite	—	—	X	—	—	X	X	X	X	X
Muscovite	—	—	X	—	—	—	—	—	—	—
Biotite	—	—	—	—	—	—	—	—	X	—
K-feldspar	—	—	—	X	—	—	—	—	—	—
Oxides	X	X	X	—	—	—	—	—	—	—

greenschists (samples L4, L5). A series of individual hydration reactions take place in the blueschist to greenschist transformation, such as:

glaucofane + epidote + quartz + H₂O → albite + actinolite + chlorite

Pressure can be estimated using the empirical geobarometer of Brown (1977). The plot of the amphiboles of samples L1 and L3 on Brown's

tentative diagram indicate pressure > 7 kbar, those of L4 and L5 (greenschist facies assemblages) indicate pressure around 3–4 kbar. These results are comparable with the analyses given by Schliestedt *et al* (1994) from the island of Kithnos.

Temperature calculated for the sample L1X using the geothermometer of Stormer (1975) is below

TABLE 2. Representative microprobe analyses of amphiboles. H₂O⁺: calculated stoichiometric H₂O content

	Sodic Amphiboles										Calcic Amphiboles					
	L1-01	L3-10	L1X-09	L1Y-17	S1X-10	S3-20	S4-08	L1X-12	L1Y-10	L4-05	L5-01	S1X-05	S3-19	S4-07		
SiO ₂	57.02	55.44	55.88	56.68	56.47	56.35	56.36	55.23	53.46	54.36	55.52	54.22	49.03	54.94		
TiO ₂	—	0.12	0.44	0.16	0.20	0.16	0.00	—	0.03	—	—	0.02	0.07	—		
Al ₂ O ₃	8.12	7.65	9.15	8.94	9.48	9.01	6.74	4.44	3.26	1.65	2.43	2.09	3.55	2.95		
Fe ₂ O ₃	3.21	3.87	2.43	2.09	2.99	2.12	3.49	3.48	1.13	1.35	1.00	0.03	3.65	1.46		
FeO	12.94	17.83	14.59	16.14	13.94	14.14	13.84	10.39	13.70	13.60	11.74	15.50	15.55	13.01		
MnO	0.31	—	0.32	0.07	0.14	0.20	0.23	0.47	0.22	0.26	—	0.15	0.28	0.36		
MgO	8.01	5.07	6.34	6.05	6.84	7.22	8.40	13.67	13.52	14.37	13.82	13.52	10.76	12.86		
CaO	1.12	0.23	0.50	0.98	0.64	0.44	2.15	10.29	11.56	11.70	11.07	11.88	10.48	9.42		
Na ₂ O	6.78	7.68	6.92	6.69	6.97	7.52	6.38	0.99	0.98	1.14	1.55	1.00	1.62	1.82		
K ₂ O	—	—	0.07	—	0.01	—	0.06	0.08	0.12	—	—	0.03	0.43	0.10		
H ₂ O	2.12	2.07	2.09	2.11	2.12	2.11	2.10	2.13	2.08	2.08	2.07	2.07	1.93	2.07		
Total	99.65	99.97	98.72	99.96	99.79	99.26	99.76	101.16	100.19	100.53	99.21	100.52	99.35	98.98		
Si ^{IV}	8.05	8.01	8.01	8.05	7.98	8.01	8.03	7.76	7.72	7.82	7.99	7.83	7.47	7.95		
Al ^{IV}	—	—	—	—	0.02	—	—	0.24	0.28	0.18	0.01	0.17	0.53	0.05		
T site	8.05	8.01	8.01	8.05	8.00	8.01	8.03	8.00	8.00	8.00	8.00	8.00	8.00	8.00		
Al ^{VI}	1.35	1.30	1.54	1.50	1.56	1.51	1.13	0.49	0.27	0.10	0.42	0.19	0.12	0.45		
Fe ³⁺	0.34	0.42	0.26	0.22	0.32	0.23	0.37	0.37	0.12	0.15	0.01	0.00	0.43	0.16		
Ti	—	0.01	0.05	0.02	0.02	0.02	0.00	—	0.00	—	—	0.00	0.01	—		
Mg	1.69	1.09	1.35	1.28	1.44	1.53	1.78	2.86	2.91	3.08	2.99	2.91	2.45	2.77		
Fe ²⁺	1.53	2.16	1.75	1.92	1.65	1.68	1.65	1.22	1.65	1.64	1.55	1.87	1.96	1.57		
Mn	0.04	—	0.04	0.01	0.02	0.02	0.03	0.06	0.03	0.03	—	0.02	0.04	0.04		
Ca	—	—	—	—	—	—	—	0.00	0.00	0.00	0.05	—	—	—		
M _{1,2,3}	5.00	5.00	5.00	5.00	5.00	5.00	5.00	5.00	5.00	5.00	5.00	5.00	5.00	5.00		
Ca	0.17	0.04	0.08	0.15	0.10	0.07	0.33	1.55	1.79	1.80	1.67	1.84	1.70	1.46		
Na	1.83	1.96	1.92	1.84	1.90	1.93	1.67	0.27	0.21	0.20	0.33	0.16	0.30	0.51		
M ₄ site	2.00	2.00	2.00	1.99	2.00	2.00	2.00	1.82	2.00	2.00	2.00	2.00	2.00	1.97		
Na	0.03	0.19	—	—	0.01	0.14	0.09	—	0.06	0.12	0.10	0.12	0.18	—		
K	—	—	0.01	—	0.00	—	0.01	0.01	0.02	—	—	0.01	0.08	0.02		
A site	0.03	0.19	0.01	—	0.01	0.14	0.10	0.01	0.08	0.12	0.10	0.13	0.27	0.02		
X _{Mg}	0.52	0.34	0.44	0.40	0.47	0.48	0.52	0.70	0.64	0.65	0.66	0.61	0.56	0.64		
X _{Fe³⁺}	0.20	0.24	0.14	0.13	0.17	0.13	0.25	—	—	—	—	—	—	—		

TABLE 3. Microprobe analyses of epidotes. H₂O⁺: calculated stoichiometric H₂O content

	BR1-04	L1X-04	L1Y-03	L1-01	L3-01	L4-04	L5-02	S1X-06	S3-09	S4-04
SiO ₂	37.52	38.78	38.38	38.56	38.13	38.13	38.33	38.08	39.06	38.39
TiO ₂	—	0.08	0.03	0.11	—	—	—	0.15	0.03	0.00
Al ₂ O ₃	21.35	24.23	24.78	23.54	21.32	22.96	24.38	23.92	24.72	24.55
Fe ₂ O ₃	15.10	12.07	11.25	12.70	14.93	13.22	11.93	12.78	12.66	11.84
FeO	—	—	—	—	—	—	—	—	—	—
MnO	0.74	0.06	0.21	0.36	—	—	—	0.05	0.19	0.12
CaO	22.06	22.91	23.61	23.29	22.93	23.33	24.08	23.39	23.50	23.12
Na ₂ O	0.32	0.15	0.02	—	—	—	—	0.03	0.17	0.14
H ₂ O	1.85	1.91	1.90	1.90	1.86	1.88	1.91	1.90	1.94	1.90
Total	98.93	100.18	100.18	100.46	99.17	99.52	100.63	100.30	102.27	100.07
12.5 oxygens										
Si ^{IV}	3.04	3.05	3.02	3.04	3.07	3.04	3.01	3.01	3.02	3.03
Al ^{IV}	—	—	—	—	—	—	—	—	—	—
Z site	3.04	3.05	3.02	3.04	3.07	3.04	3.01	3.01	3.02	3.03
Al ^{VI}	2.04	2.25	2.30	2.19	2.02	2.16	2.26	2.23	2.25	2.28
Fe ³⁺	0.92	0.71	0.67	0.75	0.90	0.79	0.71	0.76	0.74	0.70
Ti	—	0.00	0.00	0.01	—	—	—	0.01	0.00	0.00
Mn ²⁺	0.04	0.00	0.01	0.02	—	—	—	0.00	0.01	0.01
Y site	3.00	2.97	2.98	2.97	2.93	2.95	2.96	3.00	3.00	2.99
Mn ²⁺	0.01	0.00	0.00	—	—	—	—	0.00	0.00	0.00
Ca	1.91	1.93	1.99	1.97	1.98	1.99	2.03	1.98	1.95	1.95
Na	0.05	0.02	0.00	—	—	—	—	0.00	0.03	0.02
X site	1.97	1.95	2.00	1.97	1.98	1.99	2.03	1.98	1.98	1.98
Cz	67.91	75.80	77.19	73.80	69.11	73.12	76.19	74.50	75.14	76.27
Ps	30.67	24.11	22.37	25.42	30.89	26.88	23.81	25.43	24.57	23.49
Pm	1.42	0.09	0.44	0.78	—	—	—	0.08	0.28	0.24

400°C, whereas Kessel (1990) gives a temperature of about 300°C and pressure > 10 kbar for the same area.

For rocks L4 and L5 the geothermobarometer of Triboulet (1992), gives 340–360°C and 4.5–4.0 kbar respectively.

There are no indications that the prasinites studied experienced the high-pressure event (M1) that preceded the greenschist facies (M2) metamorphism of the Cyclades massif. A *P-T* path for the rocks studied consistent with the data given above (Tables 2,3,4) and the activities given by Evans (1990) indicates EBS to GS conditions under nearly isothermal uplift (Fig. 5). These results are in agreement with the *P-T* paths obtained for rocks exposed in the Cyclades (Avigad *et al.*, 1992).

The *P-T* paths in several places in the Cyclades all involve a prograde path along a cool gradient which corresponds to crustal thickening and a retrograde clockwise path which may or may not involve a temperature increase (Avigad *et al.*, 1992). It is also

remarkable that rocks which suffered heating have emerged from shallower structural levels within the Eocene orogenic wedge than rocks which suffered cooling. The boundary between these sequences strikes NE-SW (Fig. 1) and is thus perpendicular to the present strike of the Hellenic arc. This geometry is probably a result of the Oligocene-Miocene extensional tectonics which exhumed the high-pressure rocks of the Cycladic blueschist belt (Avigad *et al.*, 1992).

Furthermore, it should be kept in mind that in addition to the thermal evolution discussed above, local differences in the P_{H_2O}/P_{CO_2} ratio may also have played an important role in the stability relations among the assemblages observed in the rocks studied.

Acknowledgements

The constructive comments of an anonymous reviewer are greatly appreciated. I also acknowledge

TABLE 4. Microprobe analyses of chlorites. H₂O⁺: calculated stoichiometric H₂O content

	BR1-02	L1X-04	L1Y-03	L4-01	L5-02	S1X-02	S3-01	S4-01
SiO ₂	25.81	27.06	26.81	26.83	27.78	27.49	27.42	28.68
TiO ₂	—	0.09	0.14	—	—	0.03	0.45	—
Al ₂ O ₃	19.28	18.17	18.69	18.69	18.47	18.91	18.49	18.81
FeO	27.46	25.91	26.47	24.99	24.60	25.67	25.61	23.87
MnO	0.35	0.31	0.34	0.52	0.22	0.40	0.34	0.57
MgO	14.12	14.87	14.63	15.37	15.83	15.95	15.53	13.95
CaO	—	—	0.16	0.28	0.50	—	0.41	0.00
Na ₂ O	0.31	—	0.14	—	—	—	0.27	—
K ₂ O	—	—	—	—	—	—	—	0.59
H ₂ O	11.33	11.45	11.41	11.48	11.54	11.49	11.46	11.58
Total	98.67	97.88	98.80	98.17	98.94	99.94	99.99	98.05
14 oxygens								
Si ^{IV}	2.77	2.90	2.86	2.86	2.92	2.87	2.87	3.04
Al ^{IV}	1.23	1.10	1.14	1.14	1.08	1.13	1.13	0.96
T site	4.00	4.00	4.00	4.00	4.00	4.00	4.00	4.00
Al ^{VI}	1.21	1.20	1.20	1.21	1.21	1.20	1.15	1.38
Ti	—	0.01	0.01	—	—	0.00	0.04	—
Fe ²⁺	2.47	2.32	2.36	2.23	2.16	2.24	2.24	2.11
Mn ²⁺	0.03	0.03	0.03	0.05	0.02	0.04	0.03	0.05
Mg	2.26	2.38	2.32	2.44	2.48	2.48	2.42	2.20
Ca	—	—	0.02	0.03	0.06	—	0.05	0.00
Na	0.06	—	0.03	—	—	—	0.06	—
K	—	—	—	—	—	—	—	0.08
O site	6.04	5.94	5.97	5.96	5.93	5.96	5.98	5.83
X _{Mg}	0.48	0.51	0.50	0.52	0.53	0.53	0.52	0.51

financial support, received from the Royal Society of London and N. H. R. F.

References

- Altherr, R., Schliestedt, M., Okrush, M., Seidel, E., Krenzer, H., Harre, W., Lenz, H., Wendt, I. and Wagner, G.A. (1979) Geochronology of high-pressure rocks on Sifnos (Cyclades, Greece). *Contrib. Mineral. Petrol.*, **70**, 245–55.
- Altherr, R., Krenzer, M., Wendt, I., Lenz, H., Wagner, G.A., Keller, J., Harre, W. and Hohndozf, A. (1982) A late Oligocene / Early Miocene high temperature belt in the Attic - Cycladic Crystalline Complex (SE Pelagonian, Greece). *Geol. Jahrb.*, **E23**, 97–164.
- Andriessen, P.A.M., Boetzijk, N.A.I., Hebeda, E.H., Priem, H.N.A., Verdurmen, E.A.Th. and Verschure, R.H. (1979) Dating the events of metamorphism and granitic magmatism in the Alpine Orogen of Naxos (Cyclades, Greece). *Contrib. Mineral. Petrol.*, **69**, 215–25.
- Avigad, D. and Garfunkel, Z. (1991) Uplift and exhumation of high-pressure metamorphic terrains: the example of the Cycladic blueschist belt (Aegean sea). *Tectonophys.*, **188**, 357–72.
- Avigad, D., Matthews, A., Evans, B.W. and Garfunkel, Z. (1992) Cooling during the exhumation of a blueschist terrane: Sifnos (Cyclades, Greece). *Eur. J. Mineral.*, **4**, 619–34.
- Baltatzis, E. (1981) Contact metamorphism of a calc-silicate hornfels from Plaka area, Lavrion, Greece. *Neus. Jahrb. Mineral. Mh.*, 481–8.
- Bröcker, M. (1990) Blueschist-to-greenschist transition in the metabasites from Tinos island, Cyclades, Greece: Compositional control of fluid infiltration? *Lithos*, **25**, 25–39.
- Brown, E.H. (1977) The crossite content of a Ca-amphibole as a guide to pressure of metamorphism. *J. Petrol.*, **18**, 53–72.
- Brown, E.H. (1986) Geology of the Shuksan Suite, North Cascades, Washington, U.S.A. *Geol. Soc. Amer. Bull.*, **164**, 143–54.
- Brown, G.C., Hughes, D.J. and Esson, J. (1973) New

TABLE 5. Microprobe analyses of feldspars

	BR1-05	L1-02	L3-01	L1X-03	L1X-05	L1Y-01	L4-05	L5-02	S1X-03	S4-01
SiO ₂	68.93	68.99	68.63	68.92	64.83	69.13	69.28	68.94	68.64	69.23
TiO ₂	—	—	—	—	0.10	0.00	—	—	—	0.04
Al ₂ O ₃	19.11	18.91	19.05	19.74	17.95	19.98	19.25	19.35	19.40	19.80
FeO	—	—	—	0.38	0.11	0.20	—	—	0.08	0.16
MnO	—	—	—	—	0.03	—	—	—	0.04	0.12
CaO	—	—	—	0.13	—	0.14	—	—	0.13	0.07
Na ₂ O	11.79	11.72	11.95	11.22	0.19	10.93	11.80	11.62	11.21	11.46
K ₂ O	—	—	—	—	15.49	0.05	—	—	—	—
Total	99.82	99.62	99.63	100.37	98.70	100.44	100.33	99.91	99.50	100.88
8 oxygens										
Si	3.01	3.02	3.01	3.00	3.02	3.00	3.01	3.01	3.01	2.99
Al	0.98	0.98	0.98	1.01	0.99	1.02	0.99	0.99	1.00	1.01
Fe	—	—	—	0.01	0.00	0.01	—	—	0.00	0.01
Ca	—	—	—	0.01	—	0.01	—	—	0.01	0.00
Na	1.00	0.99	1.02	0.95	0.02	0.92	0.99	0.98	0.95	0.96
K	—	—	—	—	0.92	0.00	—	—	—	—
Ab	100	100	100	99.37	1.81	98.98	100	100	99.35	99.66
An	—	—	—	0.63	—	0.70	—	—	0.65	0.34
Or	—	—	—	—	98.19	0.33	—	—	—	—

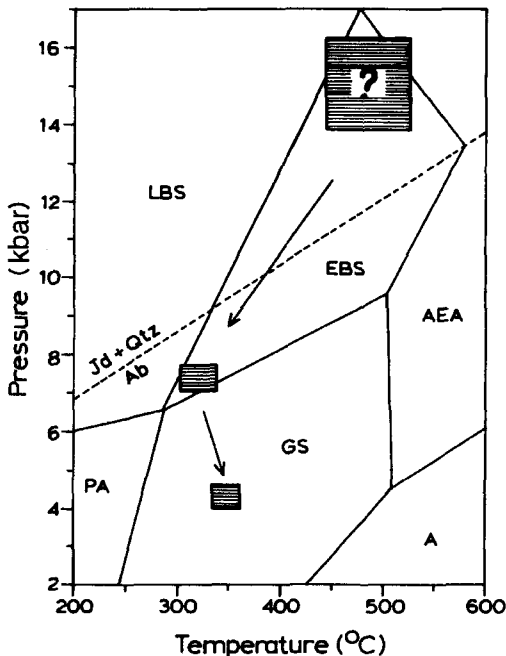


FIG. 5. Tentative pressure-temperature path for the prasinites studied. The P - T path calculated for sodic amphiboles (and co-existing minerals) whose compositions lies on the glaucophane-ferroglaucophane intersections (compositions No. 4 in Evans, 1990). The

XRF data retrieval techniques and their applications to U.S.G.S standard rocks. *Chem. Geol.*, **11**, 223–9. Dunham, A.C. and Wilkinson, F.C.F. (1978) Accuracy precision and detection limits of energy-dispersive electron-microprobe analyses of silicates. *X-ray spectrometry*, **7**, 50–6.

Dürr, St., Altherr, R., Keller, J., Okrusch, M. and Seidel, E. (1978) The Median Aegean Crystalline belt: Stratigraphy, structure, metamorphism, magmatism. In: *Alps, Apennines, Hellenides* (H. Closs, D.H. Roeder, and K. Schmidt, eds.) Schweizerbart, Stuttgart.

Evans, B.W. (1990) Phase relations of epidote-blueschists. *Lithos*, **25**, 3–23.

Kessel, G. (1990) Untersuchungen zu deformation and metamorphose in Attischen Kristallin, Griechenland. *Berliner geowiss. Abh. A*, **126**, p. 120.

Leake, B.E. (1978) Nomenclature of amphiboles. *Amer. Mineral.*, **63**, 1023–52.

Lepsius, R. (1893) *Geologie von Attika*, Berlin, 196 pp. Marinos, E.P. and Petrascheck, W.E. (1956) Lavrium.

calculation performed considered the activity of $H_2O = 0.90$. E.B.S. = epidote blueschist facies, GS = greenschist facies, A = amphibole facies, L.B.S. = lawsonite blueschist facies, A.E.A. = albite epidote amphibolite facies, P.A. = pumpellyite actinolite facies.

- Geol. Geophys. Res.*, **4**, 242 pp.
- Meschede, M. (1986) A method of discriminating between different types of mid-ocean ridge basalt and continental tholeiites with the Nb-Zr-Y diagram. *Chem. Geol.*, **56**, 207–18.
- Moore, D.E. (1984) Metamorphic history of a high-grade blueschist exotic block from the Franciscan Complex, California. *J. Petrol.*, **25**, 126–50.
- Mullen, E.D. (1983) MnO/TiO₂-P₂O₅: a minor element discriminant for basaltic rocks of oceanic environments and its implications for petrogenesis. *Earth Planet. Sci. Lett.*, **62**, 53–62.
- Pearce, J.A. (1983) Role of the sub-continental lithosphere in magma genesis at active continental margins. In: *Continental basalts and mantle xenoliths*. (C.J. Hawkesworth and M.J. Norry, eds.) Shiva, Nantwich, 230–49.
- Salemink, J. (1985) Skarn and ore formation at Serifos, Greece, as a consequence of granodiorite intrusion. *Geologica Ultrajectina*, **40**, 232 pp.
- Schliestedt, M. (1986) Eclogite-blueschist relationships as evidenced by mineral equilibria in the high-pressure rocks of Sifnos (Cyclades, Greece). *J. Petrol.*, **27**, 1437–59.
- Schliestedt, M., Altherr, R. and Matthews, A. (1987) Evolution of the Crystalline complex: petrology, isotope, geochemistry and geochronology. In: *Chemical Transport in Metasomatic Processes*. (H. C. Helgeson, ed.) Reidel Publishing Company.
- Schliestedt, M., Bartsch, V., Carl, M., Matthews, A. and Henjes-Kunst, F. (1994) The *P-T* path of greenschist facies rocks from the island of Kithnos (Cyclades, Greece). *Chem. Erde*, **54**, 281–96.
- Stormer, J.C.Fr. (1975) A practical two-feldspar geothermometer. *Amer. Mineral.*, **60**, 667–74.
- Triboulet, C. (1992) The (Na-Ca) amphibole-albite-chlorite-epidote-quartz geothermobarometers in the system S-A-F-M-C-N-H₂O. 1. An empirical calibration. 2. Applications to metabasic rocks in different metamorphic settings. *J. Metam. Geol.*, **10**, 545–56 and 557–66.

[Manuscript received 28 June 1995:
revised 3 November 1995]